Geochimica et Cosmochimica Acta 411 (2025) 173–182

Contents lists available at ScienceDirect

Geochimica et Cosmochimica Acta

journal homepage: www.elsevier.com/locate/gca

Titanium mobility and formation of anatase/pseudobrookite during diagenesis of deep-marine K-bentonites

Qian Song [a,b], Hanlie Hong [b,c,*], Kurt O. Konhauser [d], Thomas J. Algeo [c,e,f]

[a] State Key Laboratory of Loess Science, Institute of Earth Environment, Chinese Academy of Sciences, Xi'an 710061, China
[b] School of Earth Sciences, China University of Geosciences (Wuhan), Wuhan 430074 Hubei, China
[c] State Key Laboratory of Biogeology and Environmental Geology, China University of Geosciences (Wuhan), Wuhan 430074, China
[d] Department of Earth & Atmospheric Sciences, University of Alberta, Edmonton, Alberta T6G 2E3, Canada
[e] State Key Laboratory of Geological Processes and Mineral Resources, China University of Geosciences, Wuhan 430074, China
[f] Department of Geosciences, University of Cincinnati, Cincinnati, OH 45221-0013, USA

ARTICLE INFO

Associate editor: Andrew Gregory Stack

Keywords:
Elemental mobility
Alteration sequence
Volcanic ash
South China
Permian-Triassic

ABSTRACT

Titanium (Ti) is generally considered immobile in surface environments, but during diagenesis of marine sediments it has been shown be remobilized from its primary mineral phase to neoformed Ti-bearing minerals. However, the mechanisms underpinning this transformation remain poorly understood. Here, we identified two authigenic Ti-bearing minerals, anatase and pseudobrookite, within volcanic ash (K-bentonite) beds from the deep-water Upper Permian Dalong Formation to the Lower Triassic Luolou Formation at Dongpan in South China. To understand the diagenetic remobilization of Ti, we examined the K-bentonite samples by focused ion beam–scanning electron microscopy (FIB-SEM) and high-resolution transmission electron microscopy (HRTEM) to elucidate the changes in mineralogy. Anatase particles exclusively exist as single crystals (0.1–4.0 μm) or as agglomerates (0.6–15.0 μm) in association with clay minerals. Chemical compositional data show positive correlations of Ti with Ca, K, Na, and Al, which is consistent with the retention of Ti in Dongpan K-bentonites being related to adsorption of authigenic titania on clay minerals during devitrification of volcanic glass as well as to the release of Ti from detrital phenocryst grains and smectite illitization during diagenesis. The latter process was primarily mediated by porewater chemistry during diagenetic alteration. Notably, goethite and pseudobrookite are two intermediate weathering products of ilmenite in the Dongpan K-bentonites which may represent early alteration of ilmenite, whereas authigenic anatase may precipitate mainly during a later stage of early diagenesis. This finding supports that pseudobrookite can occur at low-temperature sedimentary system. Through a line scan with electron energy-loss spectroscopy (EELS), the spectra show a trend indicating that the valence state of Ti decreases from the interior of pseudobrookite to the newly formed goethite. By exploring the factors affecting Ti distribution during diagenesis, we infer that titanium can be effectively mobilized under oxidizing diagenetic conditions and subsequently reprecipitated as authigenic nano-sized TiO_2 minerals. This means that caution must be taken when using Ti to study the provenance and depositional environment of volcanic ash.

1. Introduction

Titanium occurs in various types of sedimentary rocks where it exists as an oxide mineral or sorbed to clay minerals (Spears and Kanaris-Sotiriou, 1976; Mansker et al., 1979; Schingaro et al., 2005; Hong et al., 2019). Due to its chemical inactivity and biological inertia, Ti is considered to be nearly immobile during terrestrial weathering. Consequently, in the critical zone of surface and near-surface environments, the ratio of Ti to aluminum (TiO_2/Al_2O_3) is employed as a proxy for sedimentary provenance, offering information on the weathering and depositional history of the host unit (Yamamoto et al., 1986; Wintsch and Kvale, 1994; Sugitani et al., 1996; Dai et al., 2014).

Despite the generally unreactive nature of Ti, several studies have documented that it is potentially mobile in soils and sediments, especially on micrometer to centimeter scales (Cornu et al., 1999). Large amounts of authigenic TiO_2 (titania) minerals have been identified in

* Corresponding author at: School of Earth Sciences, China University of Geosciences (Wuhan), Wuhan 430074, Hubei, China.
E-mail address: honghl8311@aliyun.com (H. Hong).

https://doi.org/10.1016/j.gca.2025.10.040
Received 24 April 2025; Accepted 30 October 2025
Available online 5 November 2025

various soils and sediments (Parnell, 2004; Fuchs et al., 2015; Schulz et al., 2016; Imperial et al., 2023), although the mechanism(s) of Ti migration and precipitation remain unclear. The fundamental structural unit of titania crystals is the titano-octahedron (Ti-O_6). Different modes of Ti-O_6 connectivity result in the formation of three types of TiO_2 crystals: rutile, anatase, and brookite. Anatase and brookite belong to a metastable state, mostly existing in low-temperature and low-pressure environments, and, thus, they are prone to transforming directly into rutile without formation of an intermediate state (Huberty and Xu, 2008; Zhang and Banfield, 2014). Authigenic titania minerals predominantly occur in the form of aggregates (0.3–150 μm), specifically anatase, in most natural environments. For example, anatase often forms in sandstone and shale that are rich in organic material and iron (Fuchs et al., 2015), located in the water–rock reaction zone (Schulz et al., 2016), and/or subjected to high thermal maturity (Schulz et al., 2016; Liu et al., 2019). Moreover, anatase is present in measurable amounts in kaolin deposits of sedimentary origin (Weaver, 1976; Baioumy, 2014). Therefore, precipitation of authigenic anatase calls into question the chemical inertness of Ti, which in turn, could result in inaccurate results when utilizing the TiO_2/Al_2O_3 ratio to determine sediment sources and stratigraphic correlations.

Previous studies of Ti mobility have focused mainly on black shales or coal-bearing sediments that are enriched in organic carbon (e.g., Parnell, 2004; Cabral et al., 2012; Schulz et al., 2016; Liu et al., 2019). Release of organic acids, e.g., humic and fulvic acids from the decomposition of organic materials, can promote degradation of Ti-bearing precursor minerals. Additionally, the complexation of dissolved Ti to organic matter facilitates the mobilization of Ti in sediments (Pe-Piper et al., 2011; Schulz et al., 2016; Liu et al., 2019). Several studies of sandstones have also identified the presence of authigenic anatase (Morad and Aldahan, 1986; Sindern et al., 2019; Imperial et al., 2023). However, to date, no consensus has been reached concerning the mobility of Ti and the environmental conditions promoting precipitation of Ti-bearing minerals in organic-poor sediments.

The Dongpan section is the best preserved marine volcanic ash deposits in southern China (He et al., 2007), having been deposited at the Permian-Triassic boundary (PTB). It is generally believed to have formed at a convergent continent margin near the southwestern South China Plate (He et al., 2014; Gao et al., 2015). Moreover, its total organic content (TOC) is lower than that of most other deep-water facies in South China (Shen, 2014), providing an opportunity to fill gaps in our understanding of Ti mobility in organic-poor systems. This is important because much of our understanding pertaining to Ti mobility is based on its complexation with organic compounds, with less understanding of whether abiotic mechanisms can also induce its mobilization. By integrating mineralogical characteristics, chemical compositions of minerals, and geochemical data for the Dongpan K-bentonite, this study explores the relationship between anatase formation, Ti mobility in K-bentonite, and the utility of ash beds for stratigraphic correlation and paleoenvironmental analysis.

2. Geological Setting and Sampling

The Dongpan section, situated at Dongpan village, Liuqiao town, Guangxi Province, southern China (GPS:22°16.20″ N, 107°41.50″ E, elevation 189 m), contains multiple volcanic ash layers deposited during the Permian-Triassic transition. Based on the occurrence of radiolarians and ostracods, the Dongpan section is regarded as a typical deep-marine facies (Fig. 1) (Feng et al., 2007; Yin et al., 2014). The Dongpan sediments consist mainly of mudstones and siltstones in the Upper Permian and siliceous mudstones in the Lower Triassic, along with 12 interbedded K-bentonite layers, which were derived from alteration of volcanic ash in a deep-marine setting (Yin et al., 2014). Previous investigations have shown that the vitrinite reflectance (Ro) of Dongpan sediments is 0.65–1.35 and the conodont color alteration index (CAI) is 2–3 (Li, 1989; Luo et al., 2011), suggesting low to moderate thermal maturity and maximum burial temperatures of ~70–120 °C (Hunt, 1996). For this study, 12 samples were collected from the Dongpan K-bentonite layers, including 9 from below the LPME, 1 from between the Late Permian Mass Extinction (LPME) and Permian-Triassic Boundary (PTB), and 2 from above the PTB, with each sample weighing approximately 500 g. The mineral composition of Dongpan section primarily consists of smectite and mixed-layer illite/smectite clays, with low contents of quartz and feldspar (Song et al., 2023). The absence of chlorite suggests that the sediments in Dongpan section formed during an early diagenetic stage because chlorite only forms in mature sedimentary rocks and deep burial environments during diagenesis or metamorphism (Hillier, 1993).

3. Methods

3.1. Major element analysis

The major element composition of the Dongpan K-bentonites was measured by wavelength-dispersive X-ray fluorescence (XRF) using a ZSXPrimusIIXRF spectrometer at the Wuhan ShangPu-spectrum Analysis Technology company. The dataset and analytical procedures were reported in Song et al. (2023).

3.2. Scanning electron microscopy (SEM)

A ~1-cm^3 aliquot of volcanic ash was taken from DP-3, DP-10 and DP-12 for SEM analysis. The surface of each aliquot was gold sprayed and then used to observe the crystallographic characteristics of minerals. However, only DP-3 yielded good results for anatase. This was also supported by the XRD results mentioned in Song et al. (2023), which showed a higher proportion of anatase at the base of the Dongpan section. The chemical composition of the Ti-bearing particles from DP-3 was determined by energy-dispersive spectrometry (EDS) during SEM analysis. Microscopic observation of anatase from DP-3 was conducted using an S-4800 cold field scanning electron microscope at the Suzhou Institute of Nano-Tech and Nano-Bionics, China Academy of Sciences. The equipment operated at an accelerating voltage of 15 kV, and the

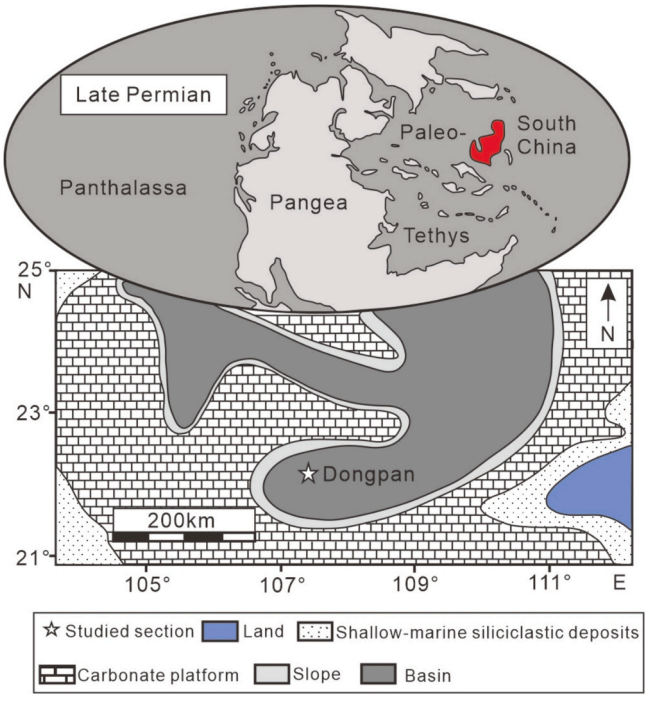

Fig. 1. Late Permian to Early Triassic palaeogeographic map showing the deep-water Dongpan section (modified after Baresel et al., 2017).

resolution of the secondary electron image was 1.0 nm.

3.3. Focused ion beam–scanning electron microscopy (FIB-SEM)

An ash sample (DP-3) was prepared as a polished thin section, which then carbon-coated to enhance its electrical conductivity for better SEM observation. The Ti-rich mineral was first found using FIB-SEM, and then an ultra-thin section of the mineral was created by *in-situ* FIB cutting. A predefined area (~20 μm^2) was coated with platinum (Pt), and the surrounding material was cut to a depth of ~10 μm using a gallium (Ga) ion beam. Afterwards, the resulting foil was picked up by EasyLift, an in-situ tungsten (W) probe inside the FIB, and then mounted on a TEM copper (Cu) grid (Omniprobe, Oxford Instrument). The extracted samples were thinned to 150 nm using a Ga ion beam at 30 kV, with beam currents ranging from 9.3nA to 80 pA and at 5 kV with a beam current of 43 pA and 2 kV with a beam current of 23 pA for the final processing. The cutting area of the ultrathin section was approximately 8 × 8 μm^2 and the total thickness was approximately 1.5 μm. Operations were performed on a ThermoFisher Scientific Helios G4 CX field-emission FIB equipped with an EDS detector and an electron backscatter diffractometer (EBSD) at the State Key Laboratory of Geological Processes and Mineral Resources of the China University of Geosciences (Wuhan).

3.4. High-resolution transmission electron microscopy (HRTEM)

The samples were ground to ~200 mesh and then the nanoparticles of TiO_2 were identified through chemical composition analysis (EDS spectra) and diffraction data. HRTEM analyses of anatase were carried out at Shanghai Institute of Metrology and Testing Technology, using FEI Tecnai G2 F20 S-TWIN with an acceleration voltage of 200 kV. The HRTEM is equipped with an EDAX solid-state EDS Detector and a Fischione high-angle annular dark-field detector (HAADF). Fast Fourier transform (FFT) was used to process the high-resolution lattice fringe image in the axis direction of the low indicating region. The chemical composition of the Ti-bearing particles was also determined by EDS during the TEM observation. The nano-sheet cut by FIB was further observed on a field-emission HRTEM at the Material and Chemical Analysis and Testing Center of the China University of Geosciences (Wuhan). The instrument operated at an accelerating voltage of 200 kV, with a point-to-point resolution $\leq$ 0.25 nm and a line resolution $\leq$ 0.12 nm. Diffraction patterns were analyzed using the Digital Micrograph software (Gatan).

3.5. Scanning transmission electron microscopy with electron energy-loss spectroscopy (STEM-EELS)

The chemical composition of a randomly chosen area from the FIB-cut section and its spectra for Ti and Fe were measured by STEM-EELS on a JEOL JEM-ARM200F scanning TEM at the Center for Electron Microscopy of Wuhan University. This instrument was equipped with a cold field-emission gun, a double spherical-aberration corrector for STEM mode, and an electron energy-loss spectrometer (EELS). The characterizations of minerals were filmed by the high-angle annular dark field (HADDF) method. The equipment operated at an accelerating voltage of 200 kV, and the resolution of STEM image was 0.078 nm. EELS line scans were recorded from the Ti-bearing minerals toward the Fe-bearing minerals, with the line evenly divided into 21 points. The energy loss near edge spectra (ELNES) of the Ti (450–475 ev), O (520–550 ev) and Fe (700–750 ev) was acquired with an exposure time of 12.0 s. Each spectrum was recorded to acquire the chemical shift and the fine structural changes in the Ti-$L_{2,3}$, O-K and Fe-$L_{2,3}$ edge profiles.

4. Results

4.1. Chemical composition analysis

EDS results of Ti-rich particles during SEM and TEM observation are shown in Tables S1 and S2. The results from SEM-EDS include the contents of Mg, K, Al, Si, Ca, Fe and Ti. Ti exhibits positive correlations with Al and Na on a Si-normalized basis (Fig. 2). TEM-EDS results include the contents of Mg, S, K, Al, Fe, Ca and Ti. Ti exhibits positive correlations with Ca and K on a Si-normalized basis (Fig. 3). All EDS data are given in the Supplementary materials (Tables S1, S2 in Supplementary Material).

4.2. SEM observations and EDS analysis

SEM-EDS results show that anatase coexists with clay minerals, characterized by high proportions of Ti, Si, O, Al and minor amounts of Fe, K, Ca (Fig. 4a-b). The elements O, Si, Al, K, Ca are consistent with the clay phases being mainly mixed-layer I/S and smectite. Minor Fe was probably derived from clay minerals and goethite, taking into account the presence of trace goethite and common incorporation of Fe in clay minerals. Anatase occurs as rounded agglomerates from 5 to 10 μm in diameter composed of tiny particles (< 1 μm), or it appears in the interlayer of clay minerals as a tetragonal crystal with a subhedral shape (~0.1 μm in size) (Fig. 4d). These observations provide clear evidence of authigenic growth.

4.3. TEM observations and EDS analysis

TEM images provide high resolution images of scattered single anatase crystals and anatase aggregates. The occurrence of anatase was identified through its electron diffraction patterns, shown in the insets of Fig. 4c-d. The symmetry and intensity distribution of the diffraction spots reflect the crystallographic symmetry and structure of the crystal. By analyzing the interplanar spacings derived from the diffraction spot separations and determining the angles between adjacent crystal planes, the mineral in Fig. 4 was identified to be anatase. Most anatase grains exhibit a euhedral tetragonal shape with sizes ranging from 100 to 500 nm (Fig. 4). Some fractions of anatase appear as subhedral tetragonal crystals with rounded edges (Fig. 4), typically ranging in size from 10 to 30 nm, which is smaller than the euhedral anatase crystals.

TEM micrographs allow for determination of the size and morphology of pseudobrookite and goethite grains (Figs. 5, 6). Euhedral pseudobrookite nanoparticles have an elongate rhombic shape with particle sizes ranging from 0.3 to 0.5 μm. Single crystals, usually consisting of microcrystal aggregates with parallel crystal faces, form elongated rhombohedral structures. Goethite often occurs in the pores surrounded by pseudobrookite and grows perpendicular to the surface of those grains. Authigenic goethite has a needle-like morphology with a crystal length of approximately 0.1 μm. Lattice images reveal the presence of intergrowths (Figs. 5c, d). The block region exhibits a *d* spacing of 2.5 Å that is vertically aligned with the larger lattice spacing of 4.9 Å (Fig. 5). The (1 1 1) *d* spacing of goethite is 2.5 Å, whereas the 4.9 Å spacing corresponds to the (200) planes in pseudobrookite. This observation shows that the host phase in these particles is pseudobrookite, and the intergrown phase is goethite. In addition to the vertical intergrowth mode, two groups of nearly parallel lattices appear at contacts between these two minerals (Fig. 5). This feature is considered to be a dislocation resulting from the attachment between crystals (De Yoreo et al., 2015). The images show an oriented attachment of goethite (yellow lines) to the surface of pseudobrookite (red lines), causing development of an edge dislocation and resulting in low-angle tilt boundaries between the two crystals. The lattice arrangement at the intersection of the two minerals is consistent and continuous, indicating a transitional growth relationship between them.

The HADDF image and elemental mapping analysis of

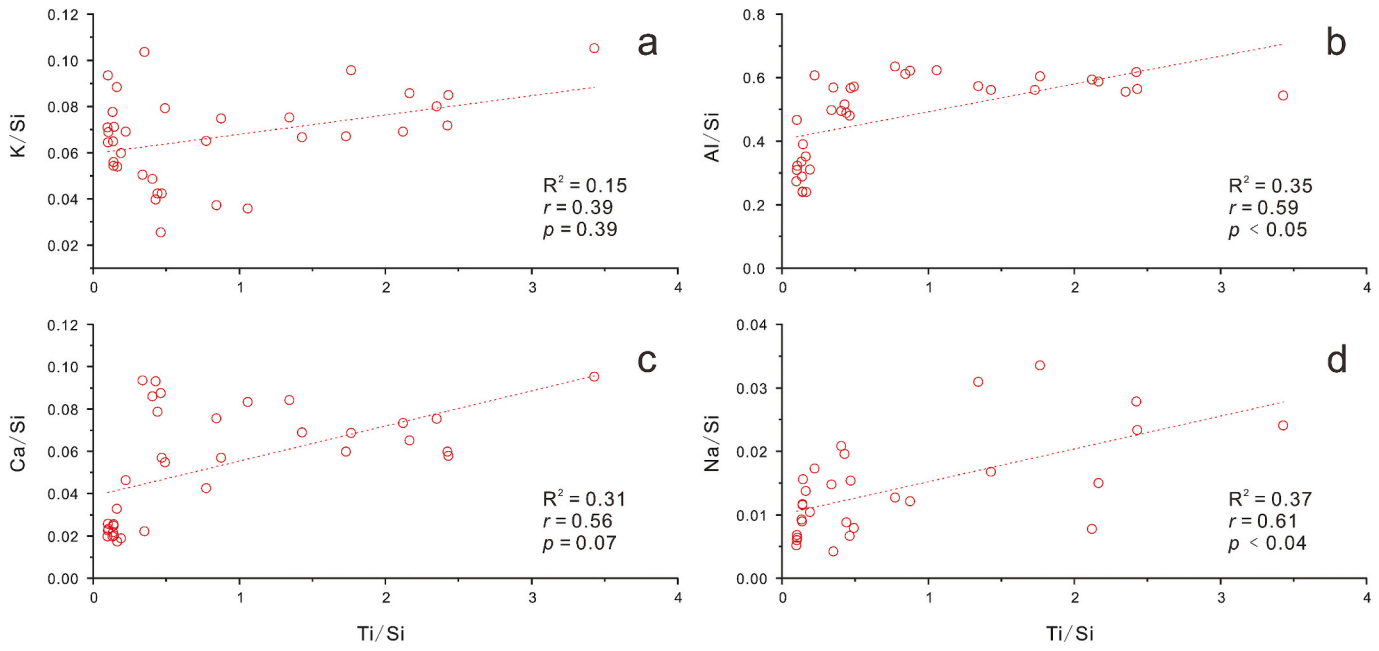

Fig. 2. Variation of K, Ca, Al, and Na versus Ti on a Si-normalized basis, from SEM-EDS analysis.

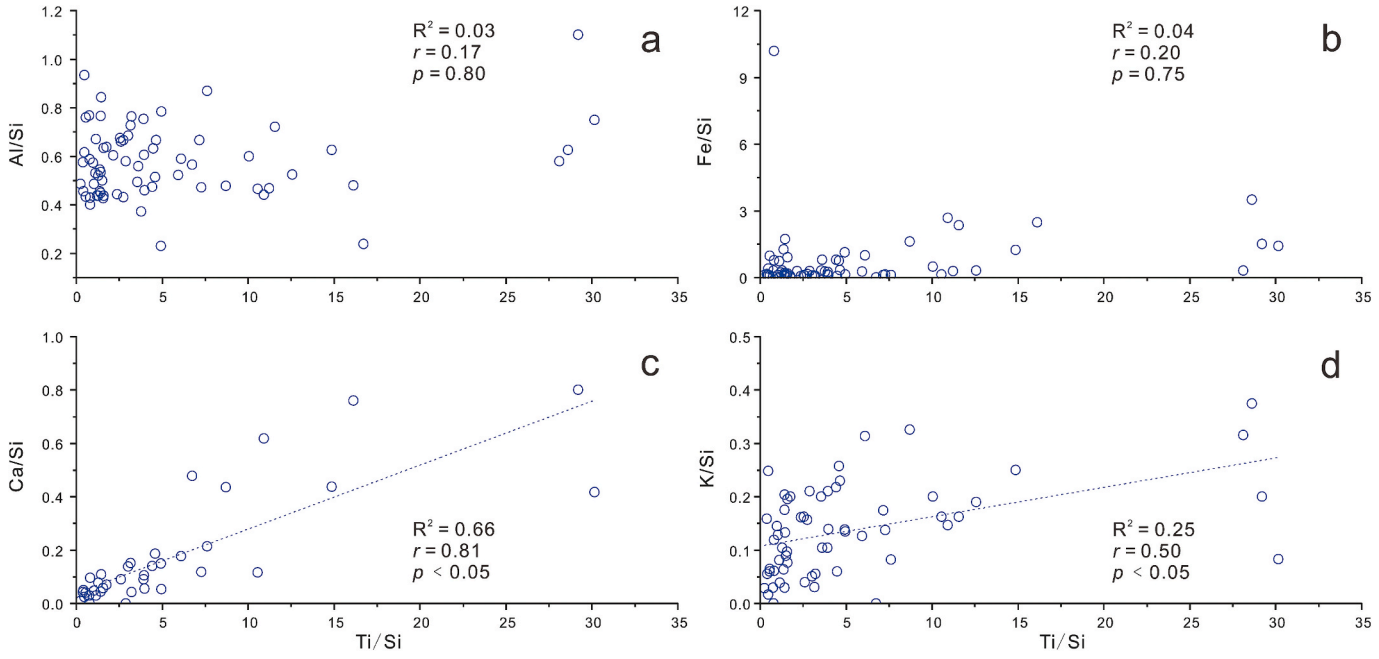

Fig. 3. Variation of Al, Ca, Fe, and K versus Ti on a Si-normalized basis, from TEM-EDS analysis.

pseudobrookite and goethite show that these minerals consist predominantly of Ti, Fe and O (Figs. 6a, d, g). The pores formed by the two minerals contain Al, Si, Mg and O (Fig. 6b-e), which indicates the presence of clay minerals.

4.4. EELS analysis

Multiple EELS spectra along a line scan are shown in the STEM image (Fig. 7), with spectra divided into three segments: pseudobrookite, goethite, and the interface between the two minerals. Within the pseudobrookite, the position of Ti-$L_{2,3}$ remains unchanged, indicating stable chemical properties (the L_2 and L_3 peak positions are 460.75 ev and 465.75 ev, representing an energy separation of 5 ev). However, at the interface of the two minerals (starting from the edge of the pseudobrookite), the position of Ti-$L_{2,3}$ shifted to lower values by ca. 1 ev, although the energy separation between the two peaks remains constant at 5 ev. Stoyanov et al. (2007) conducted a study of seven types of Ti-oxides, ranging from rutile to cubic TiO_2 structure, and concluded that with decreasing oxidation state, the position of Ti-$L_{2,3}$ shifts to lower energy levels. This relationship indicates a decrease in oxidation state from the internal region of pseudobrookite in the direction of goethite growth. The position of Fe-$L_{2,3}$ does not change; only the strength increases in the direction of goethite growth. A decrease in intensity of the oxygen peak from pseudobrookite to goethite is observed, although the position of the O-*K* edge remains unchanged (Fig. 7).

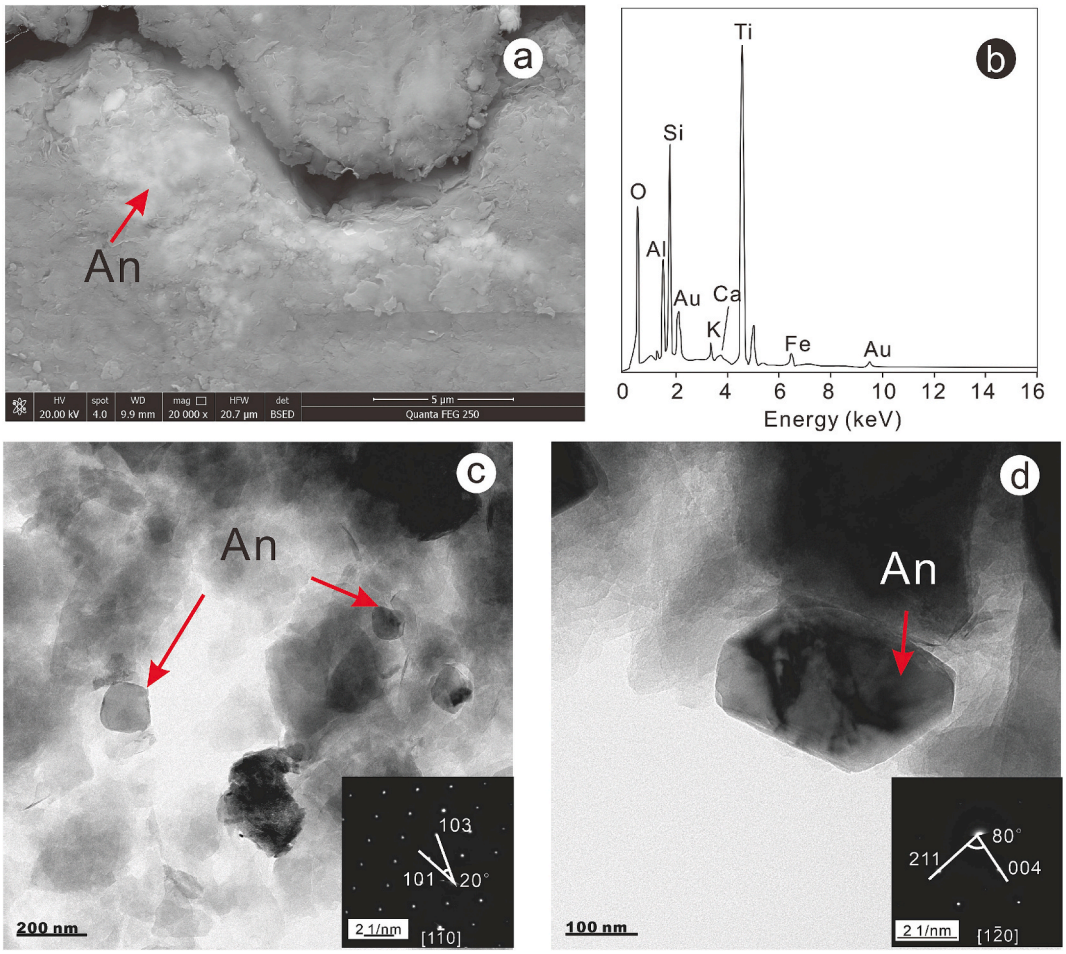

Fig. 4. Microscopic observations of authigenic anatase in Dongpan K-bentonites. (a) SEM backscattered electron image showing anatase aggregates in clay mineral matrix, and (b) the corresponding EDS spectrum showing the presence of anatase; (c) and (d): HRTEM images showing nano-scale anatase with sub-tetrahedral and truncated tetragonal bipyramidal shapes, respectively, and the corresponding electron diffraction patterns, which affirm the presence of Ti-grains of anatase; An: anatase.

5. Discussion

5.1. The mobility of Ti in marine sediments

The TiO_2/Al_2O_3 ratio is commonly used as a marker to identify material sources and to provide information on the weathering and depositional history of the host unit. However, the intensity and degree of diagenetic alteration are likely key factors controlling the migration and redistribution of Ti in the Dongpan marine sediments. The coexistence of goethite, anatase, and pseudobrookite supports the hypothesis that diagenetic alteration can lead to local Ti enrichment (Figs. 4, 5, 6). On the other hand, SEM and TEM plots show that Ti concentration is roughly correlated with the concentrations of some ionic species, e.g., Al^{3+}, Na^{+}, Ca^{2+} and K^{+} (Figs. 2, 3). XRD results reveal that the Dongpan K-bentonites consist primarily of quartz and clay minerals, with only a small amount of feldspar appearing in the lower part of the section (Song et al., 2023). Therefore, these ions are mainly derived from the interlayer sites of clay minerals such as smectite and I/S mixed-layer clays. Indeed, the correlated changes in the contents of Ti and Ca, K, Al, and Na reflect the transformations of Ti-rich minerals during clay-mineral alteration (Figs. 2, 3).

The chemical fractionation of Ti and Al during diagenetic alteration is controlled mainly by the formation of authigenic titania, i.e., the migration capacity of titanium (Liu et al., 2019; Sindern et al., 2019). Titanium was mainly incorporated into Fe-Ti aggregates and fine titania oxides, which were then diagenetically altered to authigenic Ti-oxides (Sugitani et al., 1996; Young and Nesbitt, 1998). Then, sedimentary Fe-Ti oxides, such as titano-magnetite and ilmenite, become progressively depleted in Fe and enriched in Ti. They ultimately recrystallize into pure TiO_2 minerals, thereby further sharply reducing Ti mobility (Morton and Knox, 1990; Kurtz et al., 2000). The results from both SEM and TEM indicate no correlation between Fe and Ti, which suggests that the source of Ti^{4+} in the Dongpan K-bentonites was not solely Fe-Ti-rich minerals with at least some Ti^{4+} coming from the crystal lattice of the smectite and I/S clays. Similarly, Gardner (1980) suggested that during weathering reactions, including those conserving Al, large quantities of various oxides are depleted, generating significant void space in the sediment. Authigenic titanium minerals can subsequently crystallize in the generated void space, thereby leading to chemical differentiation of Ti and Al. In addition, light rare earth elements (LREEs) have higher activities than heavy rare earth elements (HREEs) during weathering (Nesbitt, 1979; Sugitani et al., 1996; Arslan et al., 2010). As shown in Fig. 6, the Ti-rich authigenic minerals contain LREEs such as La and Ce, whereas the goethite grains contain measurable amounts of Eu. No heavy rare earth elements (HREEs) are present in either mineral (Fig. 6h to m). This observation may be explained by the mobility of Ti being similar to that of LREEs and greater than that of HREEs during mineral crystallization. This process has the potential to change the TiO_2/Al_2O_3 ratio of the sediment, even though that ratio is often considered to be fixed.

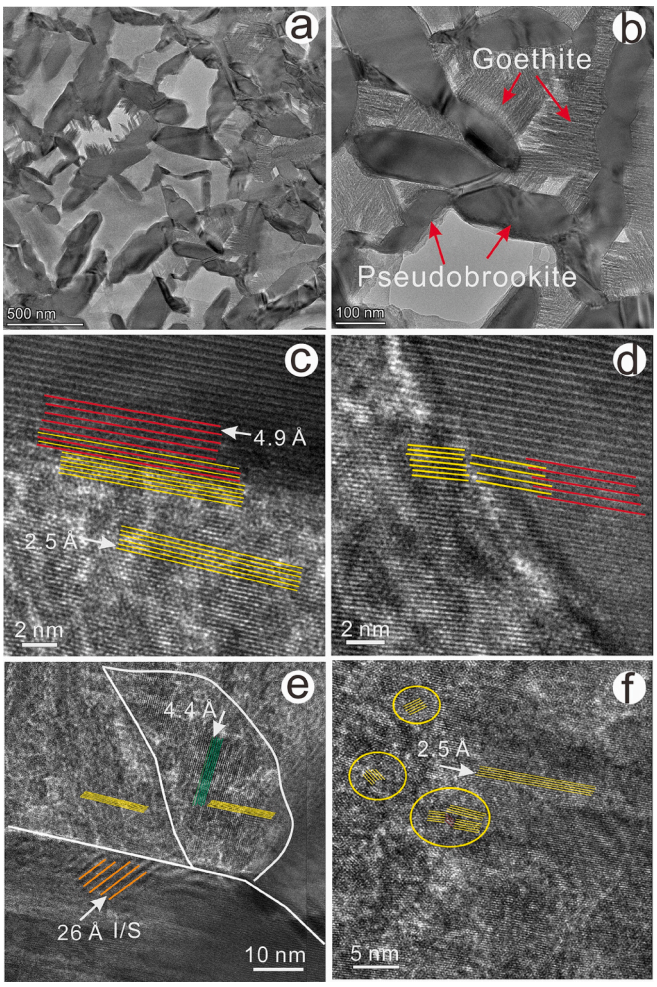

Fig. 5. (a) TEM image of Ti-bearing particles and (b) its local magnification, showing vertical growth of goethite on surfaces of pseudobrookite; (c) lattice image showing pseudobrookite (red lines, 4.9 Å spacing) and goethite (yellow lines, 2.5 Å spacing); (d) oriented attachment of goethite to pseudobrookite with creation of an edge dislocation; (e) occurrence of I/S mixed-layer clay minerals (26 Å spacing) and an intermediate phase (4.4 Å spacing) during growth of goethite from pseudobrookite; and (f) local dislocation lattice in goethite.

5.2. *Diagenetic formation of anatase in ash beds*

A titanium dioxide mineral (anatase) was found in the altered volcanic ash of the Dongpan section, the SEM and TEM results confirm the authigenic origin of anatase (Fig. 4). Highly mobile elements (e.g., Ca, Na, K and Sr) were presumably derived from labile minerals such as feldspars and micas, whereas relatively inert elements such as Ti and Fe became concentrated in refractory minerals or were absorbed by fine secondary minerals (Young and Nesbitt, 1998; Stefánsson and Gíslason,2001; Kiipli et al., 2017). The SEM results show a close association of authigenic anatase with clay minerals (Fig. 4a), providing evidence that authigenic titania formed during devitrification of volcanic glass and ash to form clay minerals.

To better constrain the migration mechanism of Ti, it is necessary to understand the genesis of authigenic titaniferous minerals. Production of anatase during alteration involves the decomposition of precursor Ti-bearing minerals, transport of Ti^{4+} ions, and secondary precipitation of anatase. Titanium is present at low concentrations in most sedimentary rocks and exists mainly in three forms: substitution in the lattice of clay minerals, uptake in primary Ti-bearing framework minerals, and neoformation of small (usually nanoscale) crystals. Some common Fe-Ti-rich minerals such as ilmenite, biotite, amphibole, leucoxene, and sphene can decompose into fine particles under diagenetic conditions. In the early diagenetic stage, authigenic titaniferous minerals may form from these minerals, primarily from igneous biotite (which may contain several weight percent of TiO_2) and less commonly from muscovite (Morad, 1988; Henry and Guidotti, 2002). These minerals decompose or become altered during diagenesis, thereby releasing Ti, which is then locally concentrated to form titania minerals. Unlike rutile, which forms at high temperatures and pressures, anatase represents a phase formed in low-temperature, low-pressure aqueous systems (Dachille et al., 1968; Hanaor and Sorrell, 2011; Galizia et al., 2016). Thus, porewater chemistry can strongly influence the growth of anatase. Early diagenetic reactions can lead to unusually high concentrations of Si, Ca and Mg to form smectite minerals. XRD results demonstrate that smectite and I/S mixed-layer minerals are the two main clay minerals in the Dongpan section, with only minor detrital components (Song et al., 2023). Previous studies have shown that smectitic minerals forming in K-bentonites via weathering of volcanic glass can incorporate trace amounts of Ti, and that structural Ti in smectite can be subsequently released during the illitization process (Papoulis et al., 2009; Fisher and Schmincke 2012; Liu et al., 2024). Positive correlations of Ti with Al, Na, K, and Ca suggest that authigenic anatase in the Dongpan K-bentonite is also related to oxidation of Ti ions released during illitization of smectite as well as weathering of detrital phenocryst grains during diagenesis (Figs. 2, 3).

The morphology of anatase is influenced by both porewater chemistry and clay mineral adsorption. TEM results show that euhedral tetragonal anatase generally has a small diameter, whereas anatase observed by SEM is usually in the form of aggregates coexisting with clay minerals and has a larger particle size. Anatase is a common trace mineral in both organic-rich and organic-poor sediments, euhedral anatase can also be found in organic-rich sediments with a tetragonal tabular shape or rounded edges (Dai et al., 2014; Liu et al., 2019). In addition, anatase often precipitates in the form of aggregates in organic-rich sediments, although this morphology is rarely seen in other environments (Schulz et al., 2016). The acidic porewater environment formed by degradation of organic materials contributes to dissolution of Ti-bearing precursor minerals in host rocks by forming stable Ti-organic complexes (Schulz et al., 2016; Liu et al., 2019), which allows subsequent transport of Ti in porewaters. However, previous studies have proven that the aggregation of anatase is independent of pH and mainly controlled by Ti complexation with organic compounds (Yang et al., 2009; Chen et al., 2012). The Dongpan K-bentonites contain relatively little organic matter, with total organic carbon (TOC) content of 0.11–0.31 % (mean 0.17 %) (Song et al., 2023). The existence of anatase aggregates (Fig. 4) in the Dongpan K-bentonites suggests that the aggregation of authigenic anatase was probably not mediated by organic matter, as it is also observed in organic-poor prodeltaic reservoir sandstones in the Scotian Basin (Imperial et al., 2023).

TEM observation shows that anatase is often produced as tiny nanoscale particles (Fig. 4c-d). Such a small size is beneficial for the migration of anatase particles in porewater and their aggregation during adsorption onto clay minerals. Aggregates are generated due to the complex reaction between organic matter and Ti in organic-rich environments (Schulz et al., 2016). However, in sediments with little organic carbon, such as sandstone and carbonate, there are few reports of aggregates. The average TOC content of Dongpan K-bentonites is 0.17 wt% (Song et al., 2023), which is lower than those typical organic rich sediments. It can be inferred that the adsorption ability of Ti by clay minerals enriched in volcanic ash should not be underestimated.

The presence of authigenic anatase in each ash layer of varying thickness in the Dongpan section suggests that the transport of Ti is a common behavior. Migration of Ti prone to happen at the minerals aggregate scale (μm – cm), which is of great importance in determining the origin of volcanic ash deposits with a thickness of only a few centimeters. Consequently, the Ti-bearing index should be carefully used

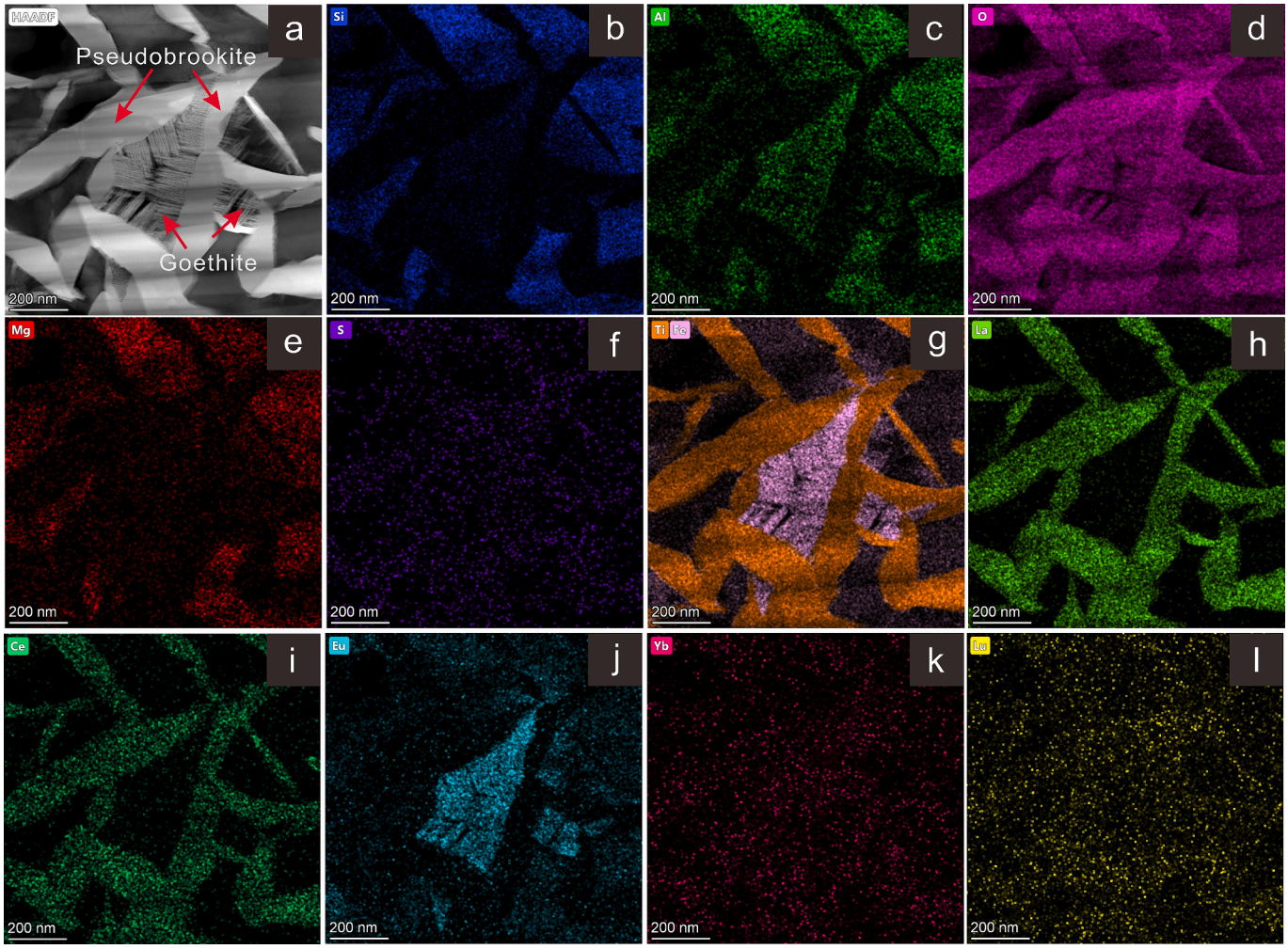

Fig. 6. Elemental maps of authigenic pseudobrookite and goethite. (a) HADDF image shows the coexistence of pseudobrookite and goethite, with corresponding distributions of (b) Si, (c) Al, (d) O, (e) Mg, (f) S, (g) Ti (orange) and Fe (pink), (h) (La), (i) Ce, (j) Eu [note: h-j are light rare earth elements], (k) Yb, and (l) Lu [note: k-l are heavy rare earth elements].

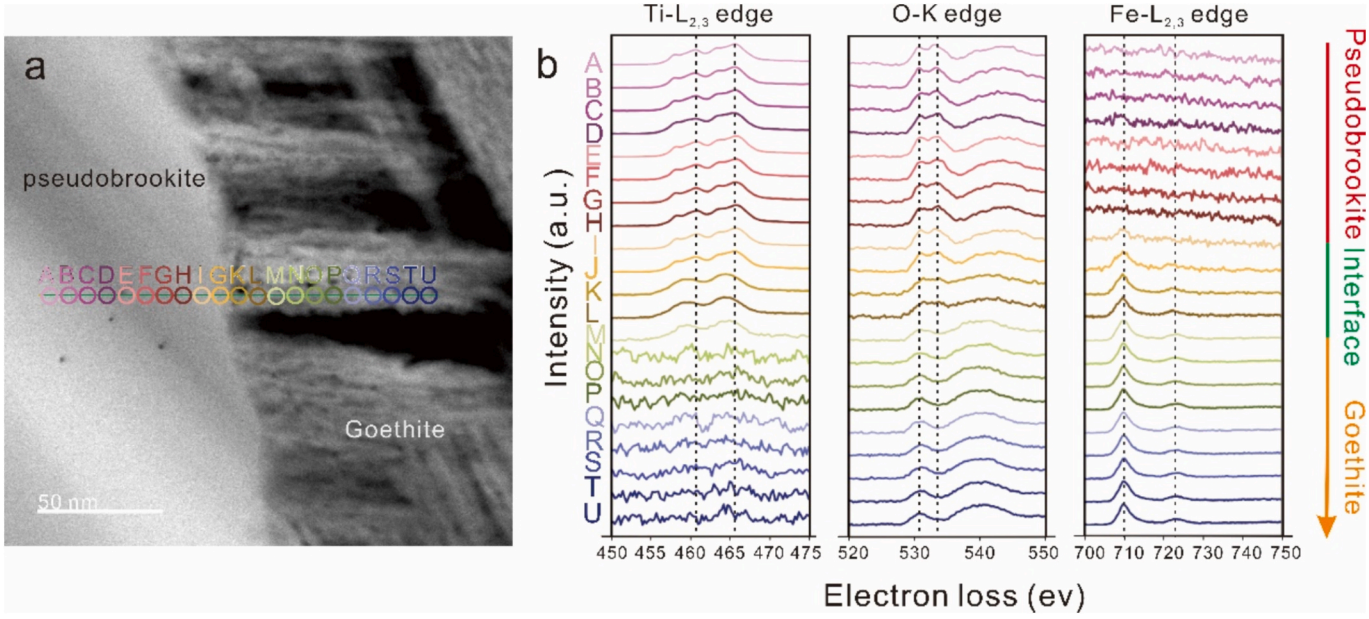

Fig. 7. HADDF image of coexisting pseudobrookite and goethite (a) and their corresponding EELS spectra of Ti-$L_{2,3}$, O-*K* edge, and Fe-$L_{2,3}$ at each analytical point (b).

when determining the source region of altered ash beds and evaluating the degree of detrital sources. A comprehensive geochemical proxy analysis method is crucial for accurately determining the source area of volcanic ash.

5.3. Alteration sequence of ilmenite in deep-marine K-bentonites

Although no relict ilmenite was detected, the Ti and Fe contents of the alteration products (Fig. 6) suggest a probable precursor in Fe-Ti oxides. Previous studies have demonstrated that the P-T K-bentonites in South China were derived from felsic igneous rocks (e.g., He et al., 2014; Zhang et al., 2021; Song et al., 2023). Ilmenite is a kind of accessory mineral commonly observed in felsic igneous rocks, and its presence in the Dongpan K-bentonites is reasonable, as also reported in K-bentonites elsewhere (Bohor and Triplehorn, 1993; Huff et al., 1998; Christidis, 2006; Huff, 2016). The absence of relict grains of ilmenite likely indicates that the chemical transformation from ilmenite to intermediate products had been completed at the initial stage of alteration. Such alteration has not been previously observed under bentonite diagenetic conditions, but analogous processes can be seen in other natural alteration systems (Grey and Reid, 1975; Morad and Adin Aldahan, 1986; Pownceby, 2010).

Many petrographic features strongly support the alteration of ilmenite during the early diagenetic process. The progressive alteration of ilmenite leads to the formation and coexistence of pseudobrookite and goethite. The coexistence of these products indicates *in situ* alteration process, as the acicular morphology of goethite (Figs. 5, 6) cannot be well-preserved during the transport. Based on the observation of FIB-TEM, the alteration of ilmenite can be divided into 2-stage process. In the initial stage of ilmenite alteration, the alteration involves the oxidation of ferrous iron, leading to the production of pseudobrookite and the leaching of Ti ion from the ilmenite lattice. The alteration reaction is shown below:

$$2Fe^{2+}TiO_3 + ½O_2 \rightarrow Fe_2^{3+}TiO_5 + TiO_2 \quad (1)$$

In the later stage of ilmenite alteration, pseudobrookite becomes unstable and can dissolve and reprecipitate to form two distinct products. During the dissolution of pseudobrookite, both iron and titanium are leached out and reprecipitated as goethite and titania (mainly anatase). The reaction is described as follow:

$$Fe_2^{3+}TiO_5 + 2H^+ + ½O_2 \rightarrow TiO_2 + 2FeOOH,$$

where the acid may come from the oxidation of Fe(II) to Fe(III) (2)

A common intermediate phase of ilmenite alteration is pseudorutile (Grey and Reid, 1975; Morad and Adin Aldahan, 1986; Pownceby, 2010). However, pseudobrookite, rather than pseudorutile, is more likely to be the product of early-stage alteration of ilmenite in volcanic ash, especially during the settling period when the internal temperature of the sediment is relatively high. Although experimental studies have demonstrated that both pseudobrookite and pseudorutile can form during alteration of ilmenite under oxic conditions, the formation of pseudobrookite under natural conditions is rarely seen. This scarcity has been attributed to pseudobrookite being a high-temperature mineral (exceeding 800 ℃), whereas pseudorutile usually forms at slightly lower temperatures ranging from 700-800 °C compared to those at which preudobrookite forms (Gupta et al., 1991). Nevertheless, TEM observations show that pseudorutile is of authigenic origin (Figs. 5, 6), and no instances of high temperature fluid/hydrothermal metasomatism events have been reported in Dongpan sediments. A study has shown that pseudobrookite can exist at ca. 120 °C, indicating that the occurrence of pseudobrookite may not be contingent on exceedingly high temperatures (Åsbrink and Magnéli, 1959).

Another line of evidence supporting the incomplete alteration of ilmenite, as shown by FIB-TEM, is the low concentration of anatase in the alteration products. Previous studies have demonstrated that the final products of ilmenite alteration are mainly rutile and hematite (Fe_2O_3) (Grey and Reid, 1975; Morad and Adin Aldahan, 1986; Gupta et al., 1991) rather than anatase (Anand and Gilkes, 1984) and goethite. Despite anatase being the earliest titanium dioxide mineral in low-temperature alteration environments (Huberty and Xu, 2008; Zhang and Banfield, 2014), and the coexistence of authigenic anatase with clay minerals (Fig. 4), the precipitation of anatase is rarely seen throughout the alteration area shown in FIB-TEM. On the one hand, the concentration of Ti ions released in the initial stage of ilmenite alteration is low (Equation (1), and as discussed above (Section 5.2), these Ti ions usually do not crystallize *in situ* immediately. Instead, they eventually precipitate within an appropriate sedimentary microenvironment through the transportation of acidic porewater or adsorption by clay minerals. On the other hand, studies have shown that the rate of pseudobrookite decomposition into its component oxides is slow at temperatures below 585℃ (Haggerty and Lindsley, 1970). Blocks of crystal planes (with spacing of 4.4 Å and 2.5 Å) and intergrowths (spacing of 4.9 Å) (Fig. 5e) suggest that, in the early stages of pseudobrookite decomposition, the Fe ions in the crystal lattice may not have been fully released, and anatase may not have yet been produced.

The precipitation of goethite from pseudobrookite may be affected by the redox state of the aqueous environment. The process of goethite formation is mainly governed by the migration of Fe ions within the lattice of pseudobrookite. Changes in the valence states of migrating cations serve as indicators of the redox conditions during particle formation or the chemical equilibrium between particles. The EELS spectra (Fig. 7) illustrate a slight decrease in the valence state of Ti ions from the interior of pseudobrookite to goethite, implying that Ti ions were reduced and Fe ions oxidized during the goethite formation from pseudobrookite. Consequently, goethite formation is favored under oxidizing conditions. In addition, conditions favorable for the precipitation of goethite are disadvantageous for precipitation of hematite. Goethite is formed via solution during partial dehydration, while hematite primarily forms through the complete dehydration of ferrihydrite aggregates (Schwertmann and Murad, 1983; Walter et al., 2001). Therefore, the observed transformation sequence of ilmenite → pseudobrookite → goethite in the Dongpan K-bentonites can be regarded as a characteristic sequence of ilmenite alteration in deep-marine systems.

6. Conclusions

The precipitation of anatase and pseudobrookite in the Dongpan K-bentonites is evidence of titanium mobility in marine porewaters. Mobilization and redistribution of Ti in sediments has the potential to alter TiO_2/Al_2O_3 ratios, thus complicating the use of this proxy for sediment provenance analysis. Chemical weathering intensity during alteration of volcanic ash is a key factor governing Ti mobility. Positive correlations of Ti with Ca, K, Na, and Al reflect a close relationship between the formation of authigenic titania and clay-mineral alteration processes. Fe-Ti oxides and Ti-bearing clay minerals are the major sources of Ti for growth of authigenic titania in the study units. Aggregation of authigenic anatase in deep-marine organic-poor environments is favored by the adsorption of Ti-nanoparticles onto clay minerals. The transformation sequence ilmenite → pseudobrookite → goethite in the Dongpan K-bentonites represents a characteristic aqueous alteration sequence for ilmenite during early diagenesis. Dissolution and reprecipitation of Fe- and Ti-oxides play an important role in the alteration of ilmenite. In addition, the widespread goethite particles on the surface of pseudobrookite suggest that the oriented aggregation mechanism of authigenic nano-goethite may be important in nature and provide evidence of intergrowth and defects in different minerals.

CRediT authorship contribution statement

Qian Song: Writing – review & editing, Writing – original draft,

Methodology, Investigation, Data curation, Conceptualization. **Hanlie Hong:** . **Kurt O. Konhauser:** Writing – review & editing, Investigation. **Thomas J. Algeo:** Writing – review & editing, Investigation.

Data availability

Data are available through Mendeley Data at https://doi.org/10.17632/dcx8z8v8ff.1.

Declaration of competing interest

The authors declare that they have no known competing financial interests or personal relationships that could have appeared to influence the work reported in this paper.

Acknowledgments

We would like to express gratitude to Q.F. for help with the HADDF photo. This work was supported by the National Natural Science Foundation of China (Project 42172045 and 42472064). The authors also wish to thank Prof. Hailiang Dong (Editor-in-Chief), Prof. Andrew G. Stack (the Associate Editor), and Dr. Georgia Pe-Piper and an anonymous reviewer for their insightful reviews, valuable comments, and suggestions.

Appendix A. Supplementary material

This supplementary material contains 2 tables. Table S1 and Table S2 show the chemical compositions of Ti-bearing minerals observed by SEM and TEM, respectively. Supplementary material to this article can be found online at https://doi.org/10.1016/j.gca.2025.10.040.

References

Anand, R.R., Gilkes, R.J., 1984. Weathering of ilmenite in a lateritic pallid zone. Clay Clay Miner. 32, 363–374.
Arslan, M., Abdìoğlu, E., Kadìr, S., 2010. Mineralogy, geochemistry, and origin of bentonite in upper cretaceous pyroclastic units of the Tirebolu area, Gìresun. Northeast Turkey. Clay Clay Miner. 58, 120–141.
Åsbrink, S., Magnéli, A., 1959. Crystal structure studies on trititanium pentoxide, Ti_3O_5. Acta Crystallogr. 12, 575–581.
Baioumy, H.M., 2014. Ti-bearing minerals in sedimentary kaolin deposits of Egypt. Appl. Clay Sci. 101, 345–353.
Baresel, B., Bucher, H., Brosse, M., Cordey, F., Guodun, K., Schaltegger, U., 2017. Precise age for the Permian–Triassic boundary in South China from high-precision U-Pb geochronology and Bayesian age–depth modeling. Solid Earth 2, 361–378.
Bohor, B.F., Triplehorn, D.M., 1993. Tonsteins: Altered volcanic-ash layers in coalbearing sequences. Geol. Soc. Am. Spec. Pap. 285, 44.
Cabral, A.R., Reith, F., Lehmann, B., Brugger, J., Meinhold, G., Tupinambá, M., Kwitko-Ribeiro, R., 2012. Anatase nanoparticles on supergene platinum–palladium aggregates from Brazil: Titanium mobility in natural waters. Chem. Geol. 334, 182–188.
Chen, G., Liu, X., Su, C., 2012. Distinct effects of humic acid on transport and retention of TiO_2 rutile nanoparticles in saturated sand columns. Environ. Sci. Technol. 46, 7142–7150.
Christidis, G.E., 2006. Genesis and compositional heterogeneity of smectites. Part III: Alteration of basic pyroclastic rocks—A case study from the Troodos ophiolite complex. Cyprus. Am. Mineral. 91 (4), 685–701.
Cornu, S., Lucas, Y., Lebon, E., Ambrosi, J.P., Luizão, F., Rouiller, J., Bonnay, M., Neal, C., 1999. Evidence of titanium mobility in soil profiles, Manaus, central Amazonia. Geoderma 91 (3–4), 281–295.
Dachille, F., Simons, P.Y., Roy, R., 1968. Pressure-temperature studies of anatase, brookite, rutile and TiO_2-II. Am. Mineral. 53 (11–12), 1929–1939.
Dai, S., Li, T., Seredin, V.V., Ward, C.R., Hower, J.C., Zhou, Y., Zhang, M., Song, X., Song, W., Zhao, C., 2014. Origin of minerals and elements in the late Permian coals, tonsteins, and host rocks of the Xinde Mine, Xuanwei, eastern Yunnan. China. Int. J. Coal Geol. 121, 53–78.
De Yoreo, J.J., Gilbert, P.U., Sommerdijk, N.A., Penn, R.L., Whitelam, S., Joester, D., et al., 2015. Crystallization by particle attachment in synthetic, biogenic, and geologic environments. Science 349 (6247), aaa6760.
Feng, Q., He, W., Gu, S., Meng, Y., Jin, Y., Zhang, F., 2007. Radiolarian evolution during the latest Permian in South China. Glob. Planet. Change. 55 (1–3), 177–192.
Fuchs, S., Schumann, D., Williams-Jones, A.E., Vali, H., 2015. The growth and concentration of uranium and titanium minerals in hydrocarbons of the Carbon Leader Reef, Witwatersrand Supergroup, South Africa. Chem. Geol. 393, 55–66.
Galizia, P., Maizza, G., Galassi, C., 2016. Heating rate dependence of anatase to rutile transformation. Process. Appl. Ceram. 10 (4), 235–241.
Gardner, L.R., 1980. Mobilization of Al and Ti during weathering—isovolumetric geochemical evidence. Chem. Geol. 30 (1–2), 151–165.
Grey, I.E., Reid, A.F., 1975. The structure of pseudorutile and its role in the natural alteration of ilmenite. Am. Mineral. 60 (9–10), 898–906.
Gupta, S.K., Rajakumar, V., Grieveson, P., 1991. Phase transformations during heating of ilmenite concentrates. Metall. Trans. B 22, 711–716.
Haggerty, S.E., Lindsley, D.H., 1970. Carnegie Inst. Wash. Year. Book 68, 247–249.
Hanaor, D.A., Sorrell, C.C., 2011. Review of the anatase to rutile phase transformation. J. Mater. Sci. 46, 855–874.
He, B., Zhong, Y., Xu, Y., Li, X., 2014. Triggers of Permo-Triassic boundary mass extinction in South China: the Siberian Traps or Paleo-Tethys ignimbrite flare-up? Lithos 204, 258–267.
He, W., Shi, G.R., Feng, Q., Campi, M.J., Gu, S., Bu, J., Peng, Y., Meng, Y., 2007. Brachiopod miniaturization and its possible causes during the Permian–Triassic crisis in deep water environments. South China. Palaeogeogr. Palaeoclimatol. Palaeoecol. 252 (1–2), 145–163.
Henry, D.J., Guidotti, C.V., 2002. Titanium in biotite from metapelitic rocks: Temperature effects, crystal-chemical controls, and petrologic applications. Am. Mineral. 87 (4), 375–382.
Hillier, S., 1993. Origin, diagenesis, and mineralogy of chlorite minerals in Devonian lacustrine mudrocks, Orcadian Basin. Scotland. Clay Clay Miner. 41 (2), 240–259.
Hong, H., Algeo, T.J., Fang, Q., Zhao, L., Ji, K., Yin, K., Wang, C., Cheng, S., 2019. Facies dependence of the mineralogy and geochemistry of altered volcanic ash beds: An example from Permian-Triassic transition strata in southwestern China. Earth Sci. Rev. 190, 58–88.
Huberty, J., Xu, H., 2008. Kinetics study on phase transformation from titania polymorph brookite to rutile. J. Solid State Chem. 181 (3), 508–514.
Huff, W.D., 2016. K-bentonites; A review. Am. Mineral. 101 (1), 43–70.
Huff, W.D., Bergstrom, S.M., Kolata, D.R., Sun, H., 1998. The lower Silurian Osmundsberg K-bentonite. Part II: Mineralogy, geochemistry, chemostratigraphy and tectonomagmatic significance. Geol. Mag. 135 (1), 15–26.
Hunt, J.M., 1996. Petroleum Geochemistry and Geology, 2nd edn. Freeman, New York, W.H, p. 743.
Imperial, A., Pe-Piper, G., Piper, D.J., Clyburne, J., 2023. The use of titania polymorphs as indicators of mesodiagenesis during hydrocarbon charge. Mar. Petrol. Geol. 149, 106075.
Kiipli, E., Kiipli, T., Kallaste, T., Pajusaar, S., 2017. Trace elements indicating humid climatic events in the Ordovician–early Silurian. Geochemistry 77 (4), 625–631.
Kurtz, A.C., Derry, L.A., Chadwick, O.A., Alfano, M.J., 2000. Refractory element mobility in volcanic soils. Geology 28 (8), 683–686.
Li, Z., 1989. Research on the maturity of organic matter and its controlling factors in the Upper Permian of the Nanpanjiang Basin. Yunnan Geology. 8, 48–57 in Chinese with English abstract.
Liu, Z.R.R., Zhou, M.F., Williams-Jones, A.E., Wang, W., Gao, J.F., 2019. Diagenetic mobilization of Ti and formation of brookite/anatase in early Cambrian black shales, South China. Chem. Geol. 506, 79–96.
Luo, G., Wang, Y., Yang, H., Algeo, T.J., Kump, L.R., Huang, J., Xie, S., 2011. Stepwise and large-magnitude negative shift in δ13Ccarb preceded the main marine mass extinction of the Permian–Triassic crisis interval. Palaeogeogr. Palaeoclimatol. Palaeoecol. 299 (1–2), 70–82.
Mansker, W.L., Ewing, R.C., Keil, K., 1979. Barian-titanian biotites in nephelinites from Oahu. Hawaii. Am. Mineral. 64 (1–2), 156–159.
Morad, S., 1988. Diagenesis of titaniferous minerals in Jurassic sandstones from the Norwegian Sea. Sed. Geol. 57 (1–2), 17–40.
Morad, S., Adin Aldahan, A.L.A., 1986. Alteration of detrital Fe-Ti oxides in sedimentary rocks. Geol. Soc. Am. Bull. 97 (5), 567–578.
Morton, A.C., Knox, R.O.B., 1990. Geochemistry of late Palaeocene and early Eocene tephras from the North Sea Basin. J. Geol. Soc. 147 (3), 425–437.
Nesbitt, H.W., 1979. Mobility and fractionation of rare earth elements during weathering of a granodiorite. Nature 279 (5710), 206–210.
Parnell, J., 2004. Titanium mobilization by hydrocarbon fluids related to sill intrusion in a sedimentary sequence. Scotland. Ore Geol. Rev. 24 (1–2), 155–167.
Pe-Piper, G., Karim, A., Piper, D.J., 2011. Authigenesis of titania minerals and the mobility of Ti: New evidence from pro-deltaic sandstones, cretaceous Scotian Basin. Canada. J. Sediment. Res. 81 (10), 762–773.
Pownceby, M.I., 2010. Alteration and associated impurity element enrichment in detrital ilmenites from the Murray Basin, southeast Australia: A product of multistage alteration. Aust. J. Earth Sci. 57 (2), 243–258.
Schingaro, E., Scordari, F., Mesto, E., Brigatti, M.F., Pedrazzi, G., 2005. Cation-site partitioning in Ti-rich micas from Black Hill (Australia): a multi-technical approach. Clay Clay Miner. 53 (2), 179–189.
Schulz, H.M., Wirth, R., Schreiber, A., 2016. Nano-crystal formation of TiO_2 polymorphs brookite and anatase due to organic—Inorganic rock–fluid interactions. J. Sediment. Res. 86 (2), 59–72.
Schwertmann, U., Murad, E., 1983. Effect of pH on the formation of goethite and hematite from ferrihydrite. Clay Clay Miner. 31 (4), 277–284.
Shen, J., 2014. Volcanic Effects to Marine Environments and Organisms Across the Permian–Triassic transition in South China. Ph.D. Dissertation, China University of Geosciences-Wuhan, 204 pp. (Chinese text with English abstract).
Sindern, S., Havenith, V., Gerdes, A., Meyer, F.M., Adelmann, D., Hellmann, A., 2019. Dating of anatase-forming diagenetic reactions in Rotliegend sandstones of the north German Basin. Int. J. Earth Sci. 108, 1275–1292.

Song, Q., Hong, H., Algeo, T.J., Fang, Q., Zhao, C., Liu, C., Xu, Y., 2023. Clay mineralogy mediated by pH and chemical weathering intensity of Permian–Triassic boundary K-bentonites at Dongpan (Guangxi, South China). Chem. Geol. 617, 121262.
Spears, D.A., Kanaris-Sotiriou, R., 1976. Titanium in some Carboniferous sediments from Great Britain. Geochim. Cosmochim. Acta 40 (3), 345–351.
Stefánsson, A., Gíslason, S.R., 2001. Chemical weathering of basalts, Southwest Iceland: Effect of rock crystallinity and secondary minerals on chemical fluxes to the ocean. Am. J. Sci. 301 (6), 513–556.
Stoyanov, E., Langenhorst, F., Steinle-Neumann, G., 2007. The effect of valence state and site geometry on Ti $L_{3,2}$ and O K electron energy-loss spectra of Ti_xO_y phases. Am. Mineral. 92 (4), 577–586.
Sugitani, K., Horiuchi, Y., Adachi, M., Sugisaki, R., 1996. Anomalously low Al_2O_3/TiO_2 values for Archean cherts from the Pilbara Block, Western Australia—possible evidence for extensive chemical weathering on the early earth. Precambr. Res. 80 (1–2), 49–76.
Walter, D., Buxbaum, G., Laqua, W., 2001. The mechanism of the thermal transformation from goethite to hematite. J. Therm. Anal. Calorim. 63, 733–748.
Weaver, C.E., 1976. The nature of TiO_2 in kaolinite. Clay Clay Miner. 24 (5), 215–218.
Wintsch, R.P., Kvale, C.M., 1994. Differential mobility of elements in burial diagenesis of siliciclastic rocks. J. Sediment. Res. 64 (2a), 349–361.
Yamamoto, K., Sugisaki, R., Arai, F., 1986. Chemical aspects of alteration of acidic tuffs and their application to siliceous deposits. Chem. Geol. 55 (1–2), 61–76.
Yang, K., Lin, D., Xing, B., 2009. Interactions of humic acid with nanosized inorganic oxides. Langmuir 25 (6), 3571–3576.
Yin, H., Jiang, H., Xia, W., Feng, Q., Zhang, N., Shen, J., 2014. The end-Permian regression in South China and its implication on mass extinction. Earth Sci. Rev. 137, 19–33.
Young, G.M., Nesbitt, H.W., 1998. Processes controlling the distribution of Ti and Al in weathering profiles, siliciclastic sediments and sedimentary rocks. J. Sediment. Res. 68 (3), 448–455.
Zhang, H., Zhang, F., Chen, J.B., Erwin, D.H., Syverson, D.D., Ni, P., Shen, S.Z., 2021. Felsic volcanism as a factor driving the end-Permian mass extinction. Sci. Adv. 7 (47), eabh1390.
Zhang, H., Banfield, J.F., 2014. Structural characteristics and mechanical and thermodynamic properties of nanocrystalline TiO_2. Chem. Rev. 114 (19), 9613–9644.